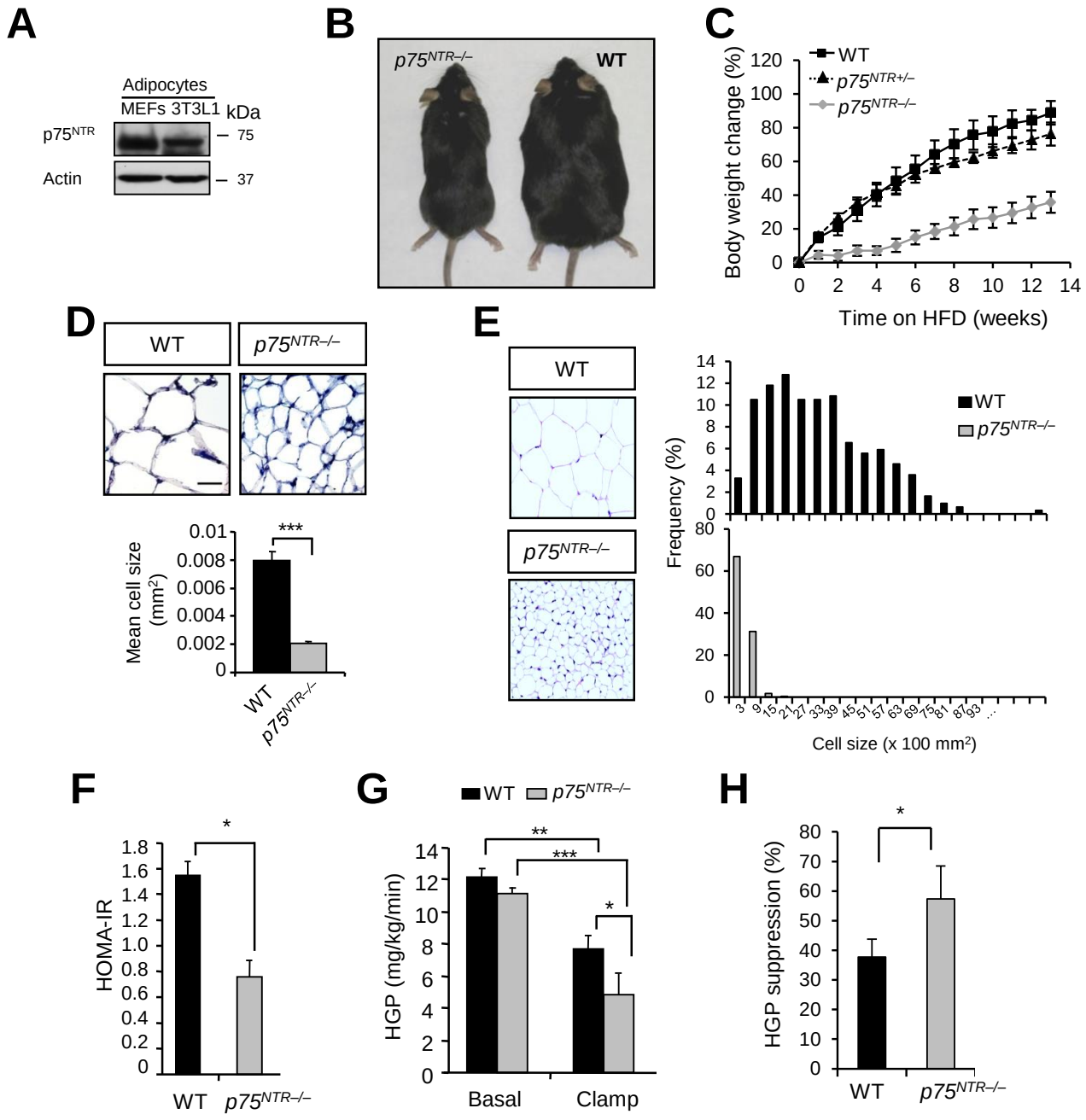

Figure S1, related to Figure 1: p75^{NTR} Deficiency Protects Mice from HFD-Induced Obesity and Insulin Resistance.

(A) p75^{NTR} protein expression in adipocyte-differentiated MEFs and 3T3L1 adipocytes. Representative immunoblot is shown from 3 independent experiments.

(B) Representative image of WT and *p75$^{NTR–/–}$* mice on HFD.

(C) Percentage of body weight change in WT (n = 7), *p75$^{NTR+/–}$* (n = 7), and *p75$^{NTR–/–}$* (n = 5) mice on HFD.

(D) Hematoxylin staining of inguinal adipose tissue sections from WT and *p75$^{NTR–/–}$* mice on HFD for 16 weeks. Quantification of adipocyte size in inguinal adipose tissue of WT and *p75$^{NTR–/–}$* mice after 16 weeks on HFD (n = 3

mice per group). Cell size from 120 adipocytes was analyzed (***$P < 0.0001$, unpaired Student's *t* test). Scale bar, 50 μm.

(E) Representative images of hematoxylin-stained paraffin-embedded epididymal adipose tissue from WT and $p75^{NTR-/-}$ mice on HFD show enlarged adipocytes in WT mice 3 weeks after HFD (left) and distribution of adipocyte size in epididymal adipose tissue of WT and $p75^{NTR-/-}$ mice after 3 weeks on HFD ($n = 10$ mice per group) (right). Cell size from 300 adipocytes was analyzed.

(F) Homeostasis model assessment of insulin resistance (HOMA-IR) in WT ($n = 5$) and $p75^{NTR-/-}$ ($n = 7$) mice on HFD (*$P < 0.05$, unpaired Student's *t* test).

(G) HGP from WT ($n = 5$) and $p75^{NTR-/-}$ ($n = 7$) mice on HFD (*$P < 0.05$; **$P < 0.01$, ***$P < 0.001$, one-way ANOVA).

(H) Percentage of HGP suppression in WT ($n = 5$) and $p75^{NTR-/-}$ ($n = 7$) mice on HFD (*$P < 0.05$, unpaired Student's *t* test).

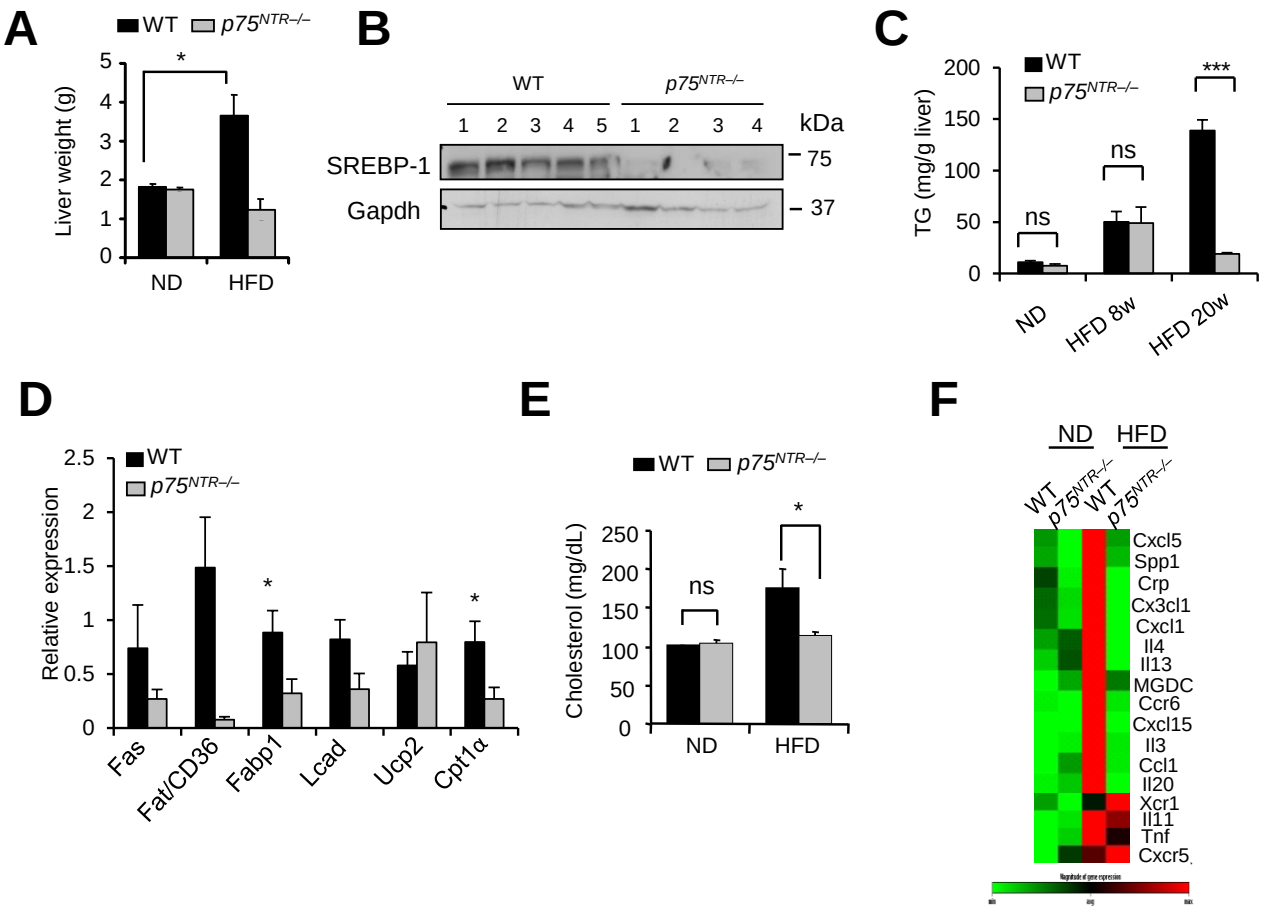

Figure S2, related to Figure 1: p75^{NTR} Deficiency Protects Mice from HFD-Induced Hepatic Steatosis, Inflammation and Increased Cholesterol.

(A) Liver weights of WT and *p75$^{NTR–/–}$* mice on ND or HFD (*P < 0.05, unpaired Student's t test; n = 3 mice per group).

(B) SREBP-1 expression in WT (n = 5) and *p75$^{NTR–/–}$* mice (n = 4) livers on HFD.

(C) Liver tryglicerides from WT and *p75$^{NTR–/–}$* mice in ND, 8 weeks, and 20 weeks on HFD (***P < 0.001, unpaired Student's t test; n = 6 mice per group).

(D) *Fas, Fat/CD36, Fabp1, Lcad, Ucp2, and Cpt1α* expression in livers from WT and *p75$^{NTR–/–}$* mice after 20 w on HFD. (**P < 0.01, *P < 0.05, unpaired Student's t test; n = 6 mice per group)

(E) Blood cholesterol levels in WT and *p75$^{NTR–/–}$* mice on HFD (* P < 0.05, unpaired Student's t test; n = 5 mice per group).

(F) Real-time PCR gene expression profiling analysis of inflammatory genes in epididymal fat pads from WT and *p75$^{NTR–/–}$* mice after 10 weeks of HFD (n = 3 mice per group).

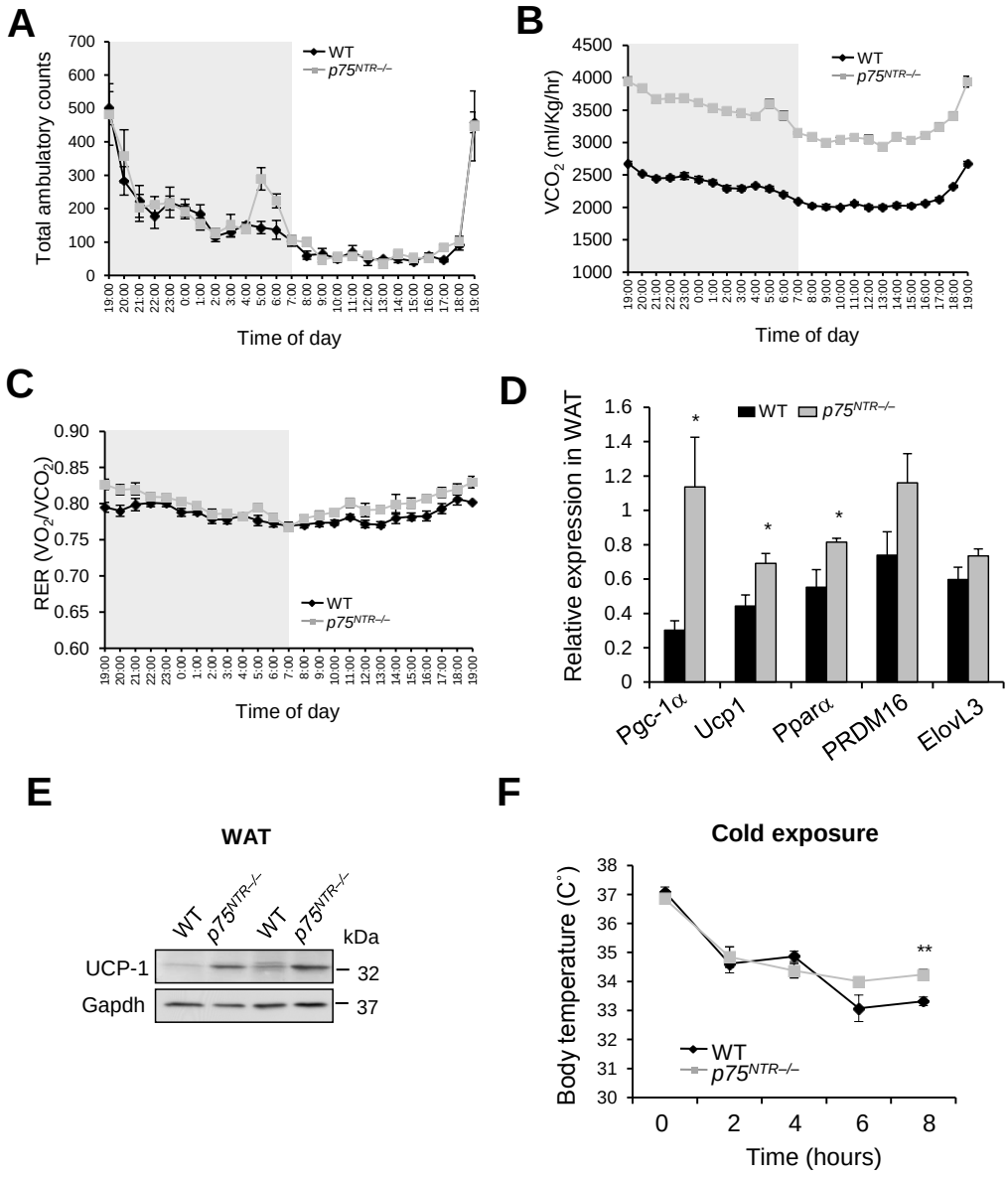

Figure S3, related to Figure 2: p75^{NTR} Deficient Mice Have Increased Metabolic Rates on HFD.

Metabolic and locomotor activity of WT mice (n = 7) and *p75$^{NTR–/–}$* mice (n = 8) over 4 days after 10 weeks of HFD. Analyses were performed of four 12-h light/dark cycles.

(A) Total ambulatory counts.

(B) Volume of CO_2 production.

(C) Respiratory exchange ratio (RER).

(D) *Pgc-1α, Ucp1, Pparα, PRDM16*, and *ElovL3* expression in WAT from WT and *p75$^{NTR–/–}$* mice on HFD (*P < 0.05, unpaired Student's t test; n = 5 mice per group).

(E) UCP1 protein expression in WAT from WT and *p75$^{NTR–/–}$* mice on HFD *(*n = 2 mice per group).

(F) Changes in rectal temperature during a cold challenge of WT and *p75$^{NTR–/–}$* mice on HFD (**P < 0.01, two-way ANOVA; n = 5 mice per group).

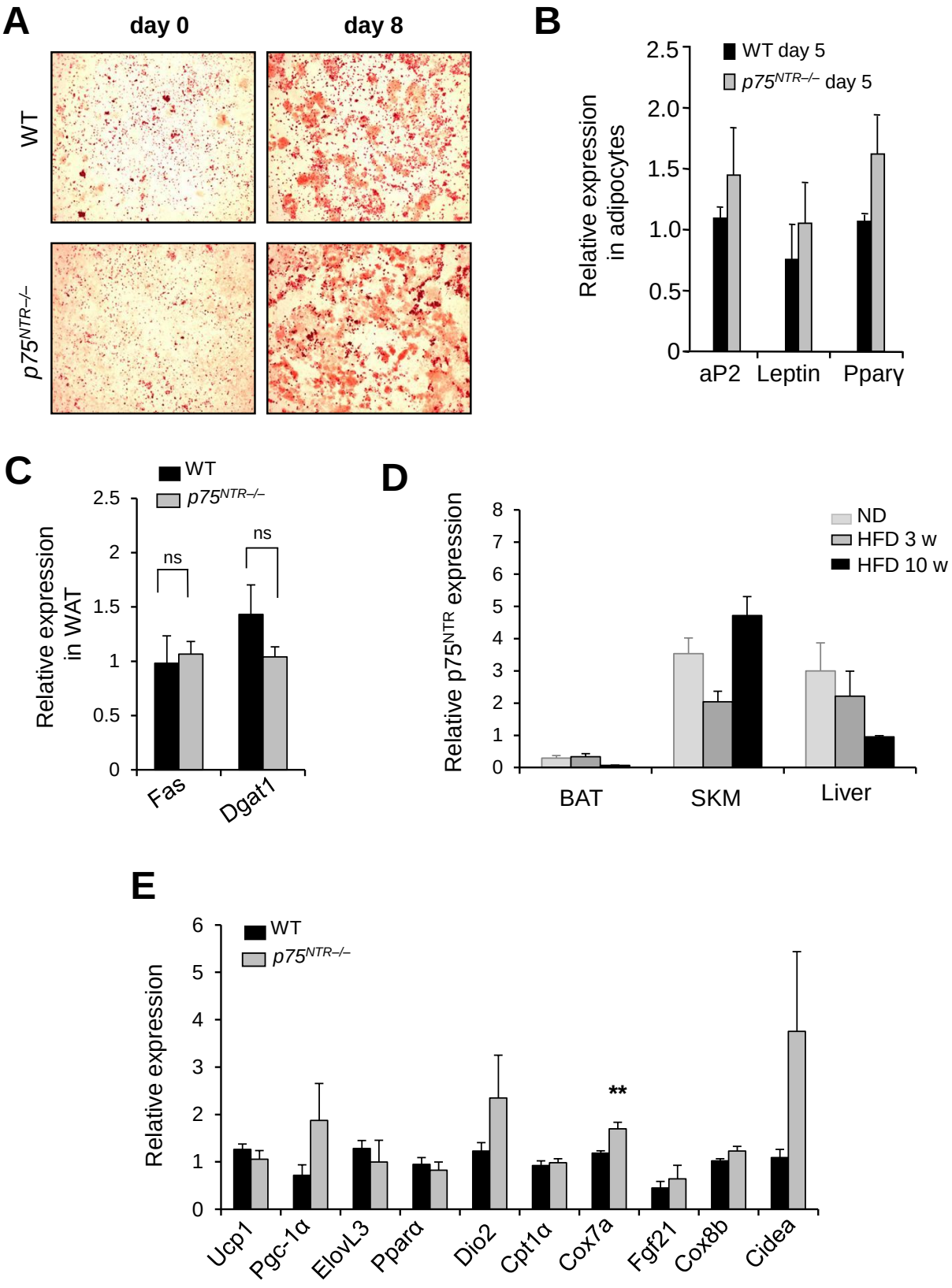
A
day 0
day 8
WT
p75NTR–/–
B
WT day 5
p75NTR–/– day 5
Relative expression in adipocytes
2.5
2.0
1.5
1.0
0.5
0
aP2
Leptin
Pparγ
C
WT
p75NTR–/–
Relative expression in WAT
2.5
2
1.5
1
0.5
0
ns
ns
Fas
Dgat1
D
ND
HFD 3 w
HFD 10 w
Relative p75NTR expression
8
7
6
5
4
3
2
1
0
BAT
SKM
Liver
E
WT
p75NTR–/–
Relative expression
6
5
4
3
2
1
0
**
Ucp1
Pgc-1α
ElovL3
Pparα
Dio2
Cpt1α
Cox7a
Fgf21
Cox8b
Cidea

Figure S4, related to Figure 2: $p75^{NTR}$ does not Regulate Adipocyte Differentiation.

(A) Representative images of Oil Red O stain from WT and $p75^{NTR-/-}$ MEFs differentiated into adipocytes. Results are from three independent experiments.

(B) *Ap2*, *leptin*, and *PPARα* RNA expression in from WT and $p75^{NTR-/-}$ MEFs differentiated preadipocytes (day 0) or fully differentiated adipocytes (day 5) (not significant, unpaired Student's *t* test). Results are from three independent experiments.

(C) *Fas* and *Dgat1* expression in WAT from WT and $p75^{NTR-/-}$ mice on HFD (not significant, unpaired Student's *t* test; $n = 5$ mice per group).

(D) $p75^{NTR}$ expression in BAT, skeletal muscle and liver from WT mice in ND, and after 3 and 10 weeks on HFD ($n = 6$ per group)

(E) *Ucp1*, *Pgc-1α, ElovL3, Pparα, Dio2, Cpt1α, Cox7a, Fgf21, Cox8b,* and *Cidea* expression in BAT from $p75^{F/F}$ ($n = 5$), Adipocyte-cre ($n = 4$), and $p75^{AKO}$ ($n = 5$) mice after 20 weeks on HFD. (**$P < 0.01$, unpaired Student's *t* test)

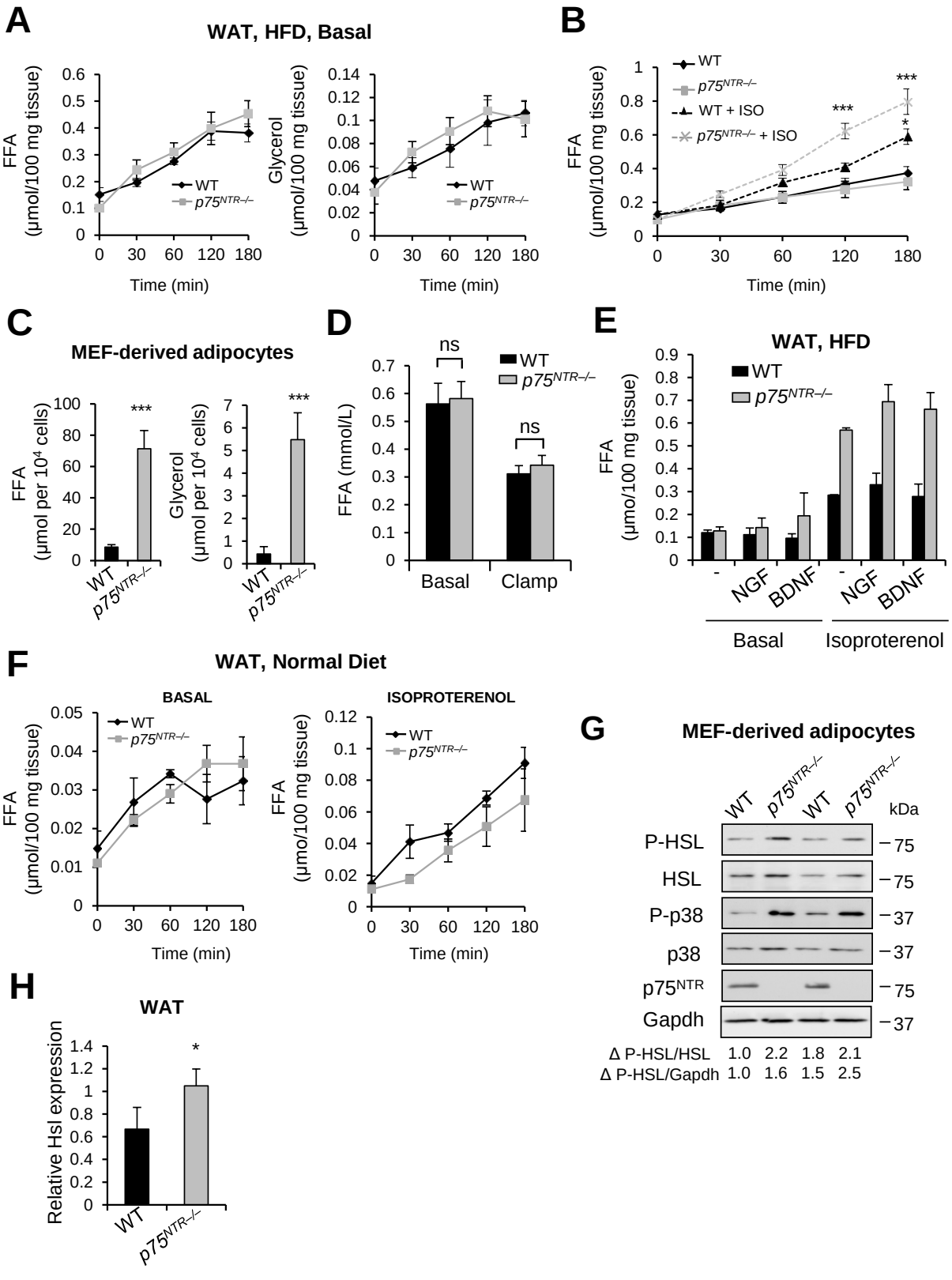
A
WAT, HFD, Basal
FFA (µmol/100 mg tissue)
Glycerol (µmol/100 mg tissue)
Time (min)
WT
p75NTR–/–
B
WT + ISO
p75NTR–/– + ISO
C
MEF-derived adipocytes
FFA (µmol per 10⁴ cells)
Glycerol (µmol per 10⁴ cells)
D
FFA (mmol/L)
ns
Basal
Clamp
E
WAT, HFD
FFA (µmo/100 mg tissue)
-
NGF
BDNF
Isoproterenol
F
WAT, Normal Diet
BASAL
ISOPROTERENOL
G
MEF-derived adipocytes
kDa
P-HSL
HSL
P-p38
p38
p75NTR
Gapdh
Δ P-HSL/HSL 1.0 2.2 1.8 2.1
Δ P-HSL/Gapdh 1.0 1.6 1.5 2.5
H
WAT
Relative Hsl expression

Figure S5, related to Figure 3: $p75^{NTR}$ Regulates Lipolysis on HFD.

(A) Basal FFA (left) and glycerol (right) levels in WAT from WT and $p75^{NTR-/-}$ mice on HFD (not significant, two-way ANOVA; $n = 8$ mice per group).

(B) Basal and isoproterenol-stimulated FFA levels in WAT from WT and $p75^{NTR-/-}$ mice on HFD (*$P < 0.05$ WT treated with isoproterenol *vs* WT basal, ***$P < 0.001$ $p75^{NTR-/-}$ treated with isoproterenol *vs* WT treated with isoproterenol, two-way ANOVA; $n = 8$ mice per group).

(C) FFA (left) and glycerol (right) levels from isoproterenol-induced WT and $p75^{NTR-/-}$ MEF-derived adipocytes (***$P < 0.001$, unpaired Student's *t* test). WT and $p75^{NTR-/-}$ MEF-derived adipocytes were incubated for 3 hours with isoproterenol. Results are from three independent experiments.

(D) FFA release in blood serum from WT ($n = 5$) and $p75^{NTR-/-}$ ($n = 7$) mice on HFD (ns, not significant; unpaired Student's *t* test).

(E) FFA from basal and isoproterenol –stimulated WAT incubated with NGF or BDNF from WT and $p75^{NTR-/-}$ mice on HFD (not significant, two-way ANOVA; $n = 2$ mice per group).

(F) Basal and isoproterenol-stimulated FFA levels in WAT from WT and $p75^{NTR-/-}$ mice on ND (not significant, two-way ANOVA; $n = 4$ mice per group).

(G) P-HSL, HSL, P-p38, p38, and $p75^{NTR}$ protein expression in in WT and $p75^{NTR-/-}$ MEF-derived adipocytes. P-HSL levels normalized to HSL and GAPDH, respectively, were quantified by densitometry (Δ represents mean value). Representative blot is shown from 3 independent experiments.

(H) *Hsl* gene expression in WAT from WT and $p75^{NTR-/-}$ mice (*$P < 0.05$, unpaired Student's *t* test; $n = 3$ mice per group).

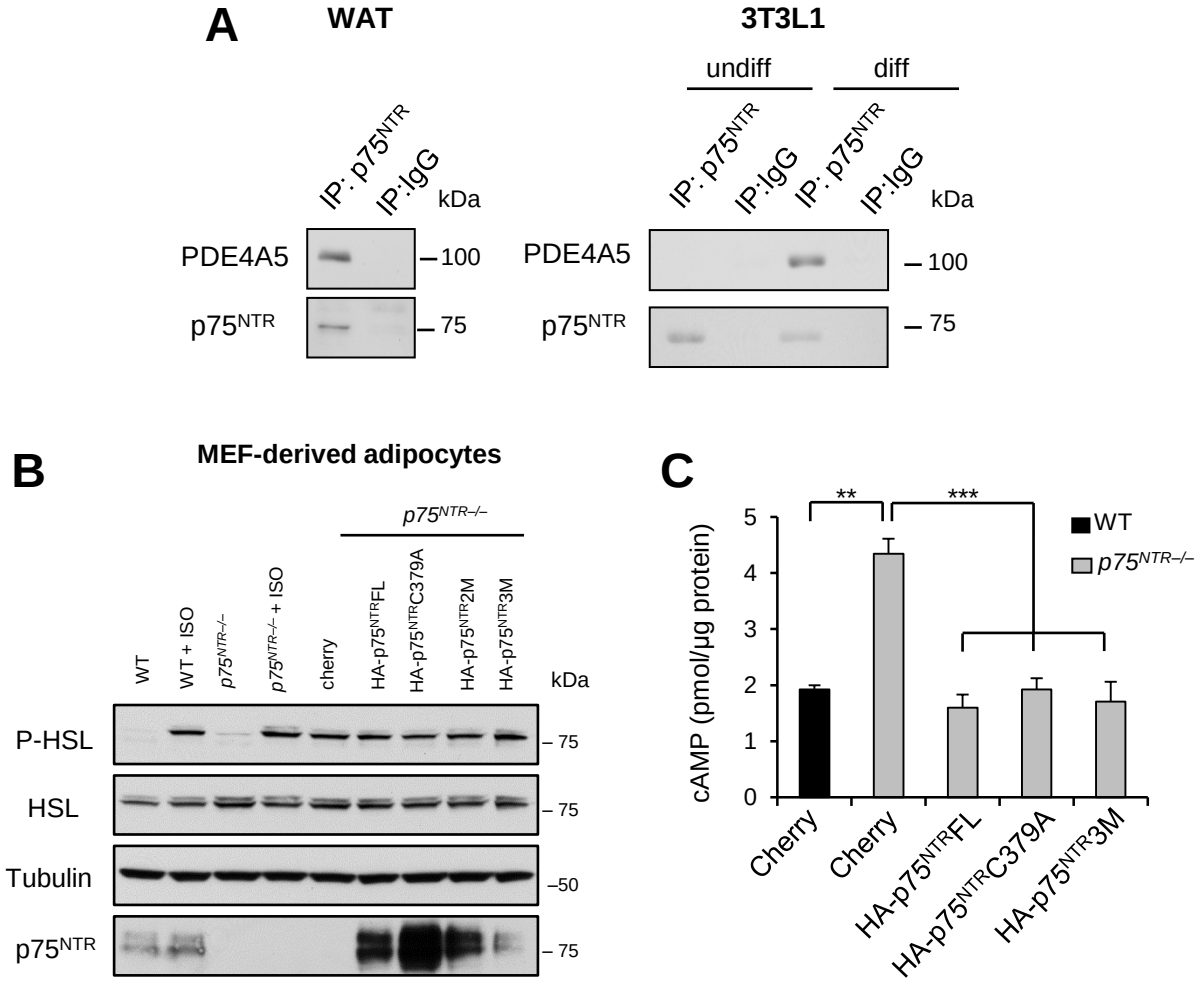

Figure S6, related to Figure 4: p75^{NTR} interacts with PDE4A5 in adipocytes.

(A) Immunoprecipitation of p75^{NTR} protein followed by western blotting to detect PDE4A5 and p75^{NTR} from WAT and 3T3L1 differentiated adipocytes. Representative immunoblot is shown from 2 independent experiments.

(B) P-HSL, HSL, and p75^{NTR} protein expression in WT and *p75$^{NTR–/–}$* MEF-derived adipocytes infected with lentiviral vectors over-expressing the indicated constructs at baseline without isoproterenol treatment. Representative immunoblot is shown from 2 independent experiments.

(C) cAMP accumulation in WT and *p75$^{NTR–/–}$* MEF-derived adipocytes infected with lentiviral vectors over-expressing the indicated constructs. (**$P < 0.01$, ***$P < 0.001$, Tukey's multiple comparisons test one-way ANOVA analysis).

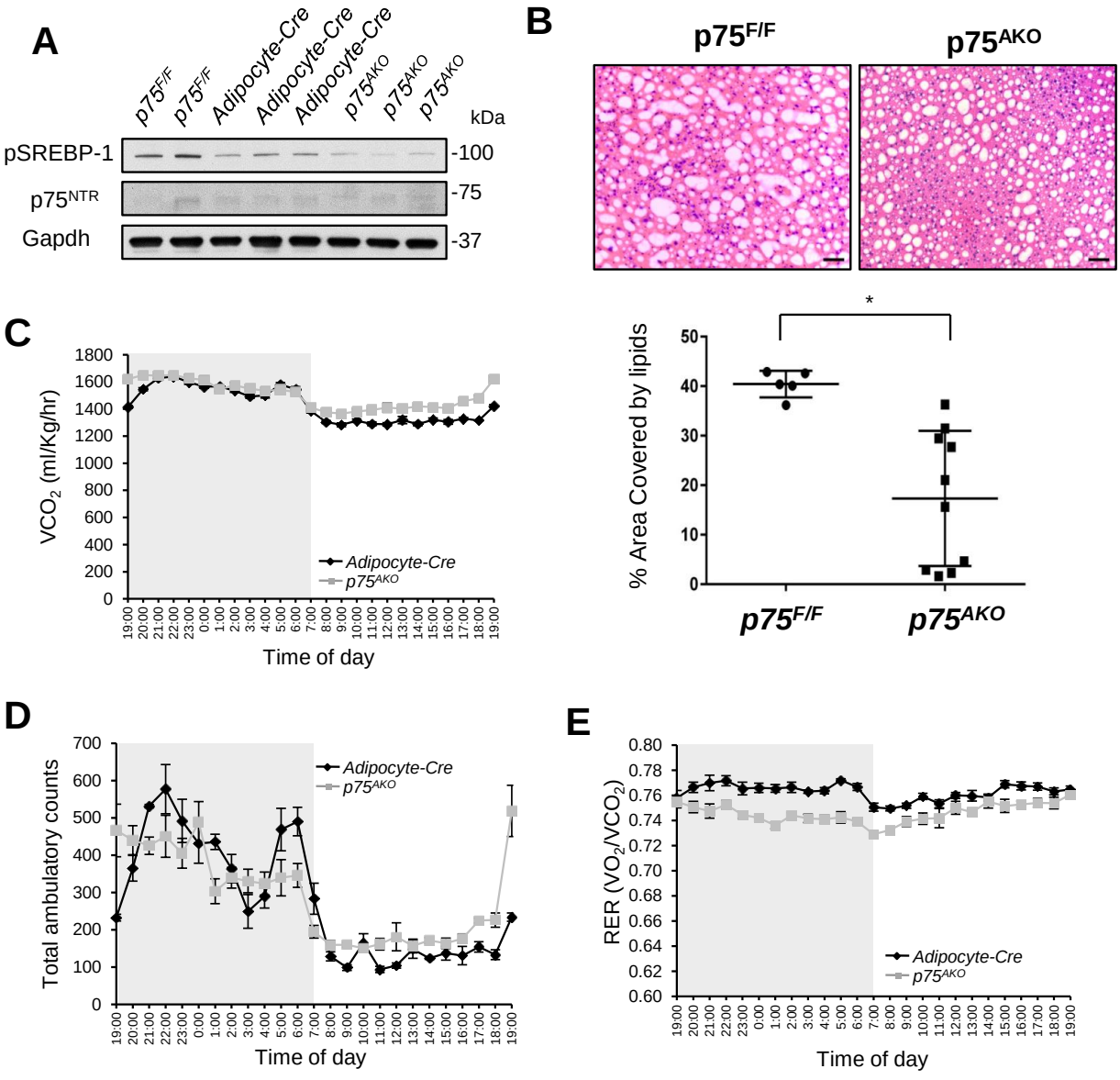

Figure S7, related to Figure 5: Loss of p75^{NTR} in the Fat Protects Mice from HFD-Induced Hepatic Steatosis and Increases Metabolic Rate in Mice after HFD.

(A) SREBP-1c and p75^{NTR} expression in liver from *p75$^{F/F}$* (*n* = 2), *Adipocyte-cre* (*n* = 3), and *p75^{AKO}* (*n* = 2) mice after 20 weeks on HFD.

(B) Representatives haematoxylin-eosin staining images from *p75$^{F/F}$* and *p75^{AKO}* livers. Dot plot representation of the percentage of area covered by lipids in livers from *p75$^{F/F}$* (*n* = 5) and *p75^{AKO}* (*n* = 10) mice after 20 weeks on HFD (*P < 0.05 by non-parametric Mann-Whitney test).

Metabolic and locomotor activity of *Adipocyte-cre* mice (*n* = 10) and *p75^{AKO}* mice (*n* = 12) over 4 days after 10 weeks of HFD. Analyses were performed of four 12-h light/dark cycles.

(C) Volume of CO_2 production.

(D) Total ambulatory counts.

(E) Respiratory exchange ratio (RER).

Supplemental Experimental Procedures

DNA constructs and viruses production. pEGFP-p75^{NTR} (GFP-p75^{NTR}) and pcDNA3.1-HA-p75^{NTR} (HA-p75^{NTR}FL) were kindly donated by Dr. Moses V. Chao. pcDNA3.1-HA- PKACα (HA-PKACα), pcDNA3.1-Myc-PKACα (Myc-PKACα), and pcDNA3.1-Myc-PKARIIβ (Myc-PKARIIβ) were used. The point mutations for constructing the HA-p75^{NTR}C379A; HA-p75^{NTR}P380A-R382A-L385A, HA-p75^{NTR}R404A-R405A-R408A were carried out using the following primers: C379A Fwd 5' CTTTACCCACGAGGCCGCACCAGTGCGAGCCCTG 3' Rev 5' CAGGGCTCGCACTGGTGCGGCCTCGTGGGTAAAG 3'; P380A-R382A-L385A Fwd 5' CCCACGAGGCCTGCGCAGTGGCAGCCCTGGCGGCCAGCTGGGGTGCCCAG 3' Rev 5' CTGGGCACCCCAGCTGGCCGCCAGGGCTGCCACTGCGCAGGCCTCGTGGG 3'; R404A-R405A-R408A Fwd 5' GCAACGCTTGATGCCCTTTTAGCCGCCCTGGCAGCCATCCAGGCAGCTGACATTGTGGAG AGTCTATGCAGCG 3' Rev 5' CGCTGCATAGACTCTCCACAATGTCAGCTGCCTGGATGGCT GCCAGGGCGGCTAAAAGGGCATCAAGCGTTGC 3'. To generate HA-p75^{NTR}P380A-R382A-L385A-R404A-R405A-R408A was carried out by using the following primers: p75^{NTR}P380A-R382A-L385A-R404A-R405A-R408A Fwd 5' CCCACGAGGCCGCAGCAGTGGCAGCCCTGGCGGCCAGCTGGGGTGCCCAG 3' Rev 5' CTGGGCACCCCAGCTGGCCGCCAGGGCTGCCATGCTGCGGCCTCGTTGGG 3'. To generate HA-p75^{NTR}C379A-P380A-R382A-L385A-R404A-R405A-R408A primers for C379A were used in the construct HA-p75^{NTR}P380A-R382A-L385A-R404A-R405A-R408A. HA-p75^{NTR}FL and all HA-p75^{NTR} mutant constructs were subcloned in a pSicoR mCherry (MP-283) lentiviral vector by PCR amplification. All constructs were confirmed by DNA sequencing. Viruses were produced by transfection of human embryonic kidney 293T cells with MP-283 and p75^{NTR} lentiviral constructs together with the packaging vector pSL4, envelope vector pSL3, and rev-regulatory vector pSL5. Viruses were subsequently concentrated from conditioned media harvested 48 and 72 h after transfection by ultracentrifugation at 25,000 rpm in a Beckman SW28 swinging bucket rotor. Viral pellet was resuspended in sterile phosphate buffered saline (PBS). MEFs-differentiated into adipocytes for 5-6 days were infected with the lentivirus for 48 hours. After, MEFs adipocytes were subjected to lipolysis assays and western blotting.

Glucose and insulin tolerance tests. Glucose and insulin tolerance tests were performed on 6 h fasted mice. For GTT, animals were injected i.p. with dextrose (1g/Kg, Hospira, Inc) whereas for ITT 0.4 units/Kg insulin (Novolin R, Novo-Nordisk) was injected i.p. Glucose excursion following injection was monitored. Blood samples were drawn at 0, 10, 30, 60 and 120 minutes after dextrose or insulin injection. Glucose was measured using a One-touch glucose-monitoring system (Lifescan).

Hyperinsulinemic-euglycemic clamp studies. Clamp studies were performed as previously described (Arkan et al., 2005; Lesniewski et al., 2007; Solinas et al., 2007). Briefly, dual jugular catheters were implanted and mice were allowed to recover three days before clamp procedure. Following 6 hours fast, an equilibrating solution (5.0 μCi/h, 0.12 ml/h [3-^{3}H]D-glucose, NEN Life Science Products) was infused into one of the jugular catheters for 90 minutes to equilibrate the plasma tracer. A basal blood sample was drawn via tail vein to obtain tracer counts for the calculation of basal glucose uptake. The insulin (8 mU/Kg/min for normal chow and 12 mU/Kg/min for HFD mice, Novo-Nordisk at a flow rate of 2 ml/min) plus tracer (0.5 μCi/h) infusion and glucose (50% dextrose, Abbot, variable rate) were initiated simultaneously, with the glucose flow rate adjusted to reach a steady state blood glucose concentration (~120 min). Steady state was confirmed by stable tracer counts in plasma during final 30 minutes of clamp. At the end of the clamp, a blood sample was taken at 110 and 120 minutes for the determination of tracer-specific activity. And at the steady state, the rate of glucose disappearance or the total GDR is equal to the sum of the rate of endogenous or HGP plus the exogenous GIR. The IS-GDR is equal to the total GDR minus the basal glucose turnover rate.

Transplants. Fat transplantation in the visceral cavity was performed as described (Tran et al., 2008) with the following modifications. Epididymal fat pads were removed from twelve week-old male WT or *p75$^{NTR-/-}$* mice. Ten

week-old male WT and *p75*$^{NTR-/-}$ mice were used as a recipient. The removed fat pads were minced and kept in saline in tubes placed in a 37°C water bath until transplantation. In anesthesized recipient mice, a total of 1 g of epididymal fat pad tissue resuspended in saline was transplanted. All animals were fed with a HFD for 12 weeks and metabolic analyses were performed. All animals were carefully examined *post-mortem* and confirmed that the implanted adipose tissue was viable.

Oil Red O and hematoxylin staining. Oil Red O and hematoxylin staining were performed according to standard protocols. Adipocyte cell size was determined using Image J software measuring at least 500 cells from each sample. Hematoxylin-eosin stainings were performed in fixed liver sections and percentage of area covered by lipids was determined with Image J software by quantifying three images per sections (four to six sections per liver).

Microscopy and image acquisition. Microscopic images were acquired with an Axioplan II epifluorescence microscope (Carl Zeiss, Inc.) and dry Plan-Neofluar objectives (10x0.3 NA, 20x0.5 NA, or 40x0.75 NA) using an Axiocam HRc CCD camera and the Axiovision image analysis software. Macroscopic images of the animals and organs were acquired with a Canon Normal EF 50 mm f/2.5 Compact Macro Autofocus Lens on a Canon EOS 10D digital camera and a Canon Macro Ring Lite Flash.

Western blotting and antibodies. Whole-cell lysates (50-200 mg) were resolved by SDS-polyacrilamide gel electrophoresis (PAGE), transferred onto a polyvinylidene difluoride (PVDF) membrane (Millipore) and incubated with the following primary antibodies: Rabbit anti-p75, 1:1000 (Millipore); mouse anti-actin, 1:10000 (Sigma); rabbit anti-SREBP1, 1:1000 (Santa Cruz Biotechnology); rabbit anti-gapdh, 1:1000 (Cell Signaling); rabbit anti-phospho-HSL, 1:1000 (Cell Signaling); rabbit anti-HSL, 1:1000 (Cell Signaling); rabbit anti-phospho-p38, 1:1000 (Cell Signaling); rabbit anti-p38, 1:1000 (Cell Signaling); rabbit anti-phospho PKA substrate, 1:1000 (Cell Signaling); rabbit anti-phospho CREB, 1:1000 (Cell Signaling); rabbit anti-CREB, 1:1000 (Cell Signaling); rabbit anti-perilipin, 1:1000 (Cell Signaling); rabbit anti-UCP-1, 1:1000 (Alpha Diagnostics); mouse anti-PKACα, 1:1000 (BD Transduction Laboratories); PKARIIα, 1:1000 (BD Transduction Laboratories); mouse anti-PKARIIβ, 1:1000 (BD Transduction Laboratories); mouse-anti-tubulin, 1:5000 (Sigma); rabbit anti-GFP, 1:1000 (Santa Cruz Biotechnology); rabbit anti-HA, 1:1000 (Abcam); mouse anti-Myc, 1:1000 (Abcam); rabbit anti-PDE4A, 1:1000 (FabGennix). Rabbit immunoglobulin G-specific horseradish peroxidase antibody or mouse immunoglobulin G-specific horseradish peroxidase (Jackson) was used for detection. Quantification was performed on the Scion NIH Imaging Software. Representative western blots from three independent experiments are shown.

Gene expression analysis. RNA extraction, reverse transcription and real-time PCR were performed as described (Passino et al., 2007). Gene expression profiling using PCR arrays was performed using RT^2 Profiler^{TM} PCR Array for inflammatory Cytokines and Receptors kit (SABiosciences) according to the manufacturer's instructions. For these profiling experiments, RNA was reverse transcribed to cDNA by using the RT^2 First Strand Kit (SABiosciences) according to manufacturer's instructions. Primers used were: Acc: Fwd 5' TAAACCAGCACTCCCGATTC, Rev 3' CCAGAGATCCCCAAATCAGA; Ap2: Fwd 5' GGA ACC TGG AAG CTT GTC TCC 3', Rev 5' ACC AGC TTG TCA CCA TCT CG 3'; Cidea: Fwd 5' GCAGCCTGCAGGAACTTATC, Rev 3' CCATTTCTGTCCCTTTTCCA; Cox7a: Fwd 5' AAAACCGTGTGGCAGAGAAG, Rev 3' CCAGCCCAAGCAGTATAAGC; Cox8b: Fwd 5' TGCGAAGTTCACAGTGGTTC, Rev 3' TGCTGCGGAGCTCTTTTTAT; Cpt1α: Fwd 5' TCCATGCATACCAAAGTGGA, Rev 3' TGGTAGGAGAGCAGCACCTT; Dgat1: Fwd 5' GGCCCAAGGTAGAAGAGGAC 3', Rev 5' GATCAGCATCACCACACACC 3'; Dio2: Fwd 5' CCA CCT GAC CAC CTT TCA CT 3', Rev 5' TGG TTC CGG TGC TTC TTA AC 3'; Elovl3: Fwd 5' GGATGACGCCGTAGTCAGAT 3', Rev 5' GAATGGACGCCAAAGTTCAT 3'; Fabp1: Fwd 5' CATCCAGAAAGGGAAGGACA, Rev 3' TTTTCCCCAGTCATGGTCTC; Fas: Fwd 5' TTGCTGGCACTACAGAATGC 3', Rev 5' AACAGCCTCAGAGCGACAAT 3'; Fat/CD36: Fwd 5' TGCTGGAGCTGTTATTGGTG, Rev 3' TGGGTTTTGCACATCAAAGA; Fgf21: Fwd 5'

CTGGGGGTCTACCAAGCATA, Rev 3' CACCCAGGATTTGAATGACC; Gapdh: Fwd 5' CAA GGC CGA GAA TGG GAA G 3', Rev 5' GGC CTC ACC CCA TTT GAT GT 3'; Hsl: Fwd 5' AGA CAC CAG CCA ACG GAT AC 3', Rev 5' ATC ACC CTC GAA GAA GAG CA 3'; Lcad: Fwd 5' GAAGCAGTACCAGGCCTCAG, Rev 3' GACACTCTTTGGGGTGGAAA; Leptin: Fwd 5' CCA AAA CCC TCA TCA AGA CC 3', Rev 5' GTC CAA CTG TTG AAG AAT GTC CC 3'; Pgc1: Fwd 5'TATGGAGTGACATAGAGTGTGCT 3', Rev 5'CCACTTCAATCCACCCAGAAAG 3'; Ppar: Fwd 5'AGAGCCCCATCTGTCCTCTC 3', Rev 5' ACTGGTAGTCTGCAAAACCAAA 3'; Ppar: Fwd 5' GGA AAG ACA ACG GAC AAA TCA 3', Rev 5' ATC CTT GGC CCT CTG AGA; PRDM16: Fwd 5' TTCCAATCCCACCAGACTTC 3' TG 3', Rev 5' CAGCATCTCCCATCCAAAGT 3'; Ucp1: Fwd 5' AGG CTT CCA GTA CCA TTA GGT 3', Rev 5' CTG AGT GAG GCA AAG CTG ATT T 3', and $p75^{NTR}$ was determined using oligonucleotides obtained from SABiosciences.

Lipolysis and palmitic acid oxidation. Lipolysis studies were performed in explants from freshly epididymal fat pads (± 20 mg) and in MEFs differentiated into adipocytes as described (Jaworski et al., 2009). Explants were incubated with DMEM with or without 200 nM isoproterenol (Sigma) and free fatty acids and glycerol were measured following manufacturer's instructions (Zenbio). 20 μM of H-89 (Cell Signaling) was added 1 hour prior isoproterenol stimulation. 100 ng of NGF (Peprotech) and 50 ng of BDNF (Peprotech) were added for 3 hours. Isolated primary adipocytes were used to measure palmitic acid oxidation as described (Jaworski et al., 2009). Briefly, adipocytes were isolated and palmitate oxidation was measured by the production of $^{14}CO_2$ from [1-^{14}C]palmitic acid (0.2 μCi/ml) with unlabelled palmitate present in the medium. Cells were incubated for 2-3 hours containing a piece of filter paper moistened with 0.1N KOH. After incubation, medium was acidified with 0.5M of H_2SO_4, and tubes were maintained seal for an additional 1 hour. After filter papers were removed and transferred into scintillation vials for radioactive counting.

$p75^{NTR}$ ELISA assays. His-HSP20 and His-$p75^{NTR}$ICD were purified as described (Sin et al., 2011). Both were diluted to a final concentration of 256 nmol/l in coating buffer (TBS with 1 mM DTT, 0.6 mM PMSF, Roche Complete protease inhibitor cocktail) and 20 μl were added to the wells of a 384-well low-flange, white flat bottom polystyrene high-bind microplate (Corning). Plates were incubated 1 h at room temperature. Protein solution was removed from the plate and 100 μl blocking buffer (TBS with 0.03% milk powder, 1 mM DTT, 0.6 mM PMSF, 0.05% Tween 20) was added to each well. Plates were incubated at room temperature for 1 h. Blocking buffer was removed, and serial dilutions of His-PKA-Cα or PKA-RIIb with concentrations between 128 and 8192 nM were added to the wells. Control wells with only blocking buffer added were also included. Plates were incubated for 2 h at room temperature, then washed three times with TBS with 0.05% Tween-20 (TBS-T). For quantification of bound PKA subunits, mouse PKA-Cα or -RIIβ-specific antibodies (BD Biosciences 610981 or 610626, respectively) were added in 1:1000 dilution in blocking buffer (20 μl/well) and incubated for 1 h at room temperature. Wells were washed three times with TBS-T, and an anti-mouse-HRP conjugate antibody (GE Healthcare, NXA931) was added in 1:5000 dilution, 20 μl/well, and incubated for 1 h at room temperature. For detection, wells were washed as before and each filled with 20 μl ECL Western blotting substrate solution (Pierce) before being read on a Mithras LB 940 platereader (Berthold). The results were plotted usingGraphPad Prism software. Kd values were estimated by fitting a hyperbolic binding curve using nonlinear regression and a one site binding model in GraphPad Prism 5.

Peptide array mapping. Peptide libraries were synthesized by automatic SPOT synthesis (Frank, 2002). Synthetic overlapping peptides (25 amino acids in length) of human $p75^{NTR}$ intracellular domain (ICD) were spotted on Whatman 50 cellulose membranes according to standard protocols by using Fmoc-chemistry with the AutoSpot Robot ASS 222 (Intavis Bioanalytical Instruments). The interactions of spotted peptides with His-PKACα and PKARIIβwere determined by overlaying the membranes with 10 μg/ml recombinant protein overnight at 4 C. Bound RIIβ protein was detected as in the ELISA (see above), and bound PKACα with an anti-His-HRP conjugate (Qiagen, 1014992), and detection was performed using ECL reagent (Pierce) and X-ray films (Kodak). Alanine scanning was performed as described previously (Bolger et al., 2006).

Core body temperature. Core body temperature was measured rectally with a digital thermometer (model 4600; Yellow Springs Instruments).

Cell culture and primary adipocyte isolation. 3T3L1 cells were maintained in DMEM containing 10% bovine serum. MEFs derived from embryos of WT and *p75*$^{NTR-/-}$ mice and HEK293T cells were cultured in DMEM with 10% heat-inactivated fetal bovine serum (FBS). All media were supplemented with 1% penicillin/streptomycin (Invitrogen). Isolation of MEFs was performed as previously described (Conner, 2001). Briefly, embryos were isolated at E12-E14, the heads and internal organs were removed, and the remaining embryo was minced with scissors and kept on ice in PBS. Minced embryos were centrifuged for 5 min at 500 X *g* and trypsinized for 20 min at 37°C with occasional shaking with 1X Trypsin-EDTA. Trypsin was deactivated by the addition of DMEM with 10% FBS. MEFs were then pelleted by centrifugation at 500 X *g* for 5 min. Pellets were resuspended in DMEM with 10% FBS and then poured through a 70 μm filter onto a 10 cm culture plate. Differentiation of 3T3L1 cells and MEFs was performed as described (Le Moan et al., 2011). Briefly, differentiation was induced by incubating confluent monolayers for 3 days in DMEM containing 10% FBS, 0.5 mM 3-isobutyl-1-methylanthine, 0.4 μg/mL dexamethasone, 1 μg/mL of insulin, and 5 μM of Rosiglitazone. Medium was replaced every 2 days with DMEM containing 10% heat-inactivated FBS and 1 μg/mL of insulin. Isolation of primary adipocytes was performed as described (Viswanadha and Londos, 2006). Briefly, epididymal fat pads were obtained from mice on normal diet (ND), then mixed and minced in Krebs-Ringer Bicarbonate-Hepes (KRBH) buffer, pH 7.4, containing 10 nM bicarbonate, 30 mM Hepes, 200 nM adenosine, 2.5 mM glucose and 1% fatty-acid free BSA. Collagenase (Invitrogen) was added and incubated for 40 minutes. Mixture was filtered through a nylon strainer and centrifuged at 400 X *g* for 1 minute.

Supplemental References

Arkan, M. C., Hevener, A. L., Greten, F. R., Maeda, S., Li, Z. W., Long, J. M., Wynshaw-Boris, A., Poli, G., Olefsky, J., and Karin, M. (2005). IKK-beta links inflammation to obesity-induced insulin resistance. Nat Med *11*, 191-198.

Bolger, G. B., Baillie, G. S., Li, X., Lynch, M. J., Herzyk, P., Mohamed, A., Mitchell, L. H., McCahill, A., Hundsrucker, C., Klussmann, E., *et al.* (2006). Scanning peptide array analyses identify overlapping binding sites for the signalling scaffold proteins, beta-arrestin and RACK1, in cAMP-specific phosphodiesterase PDE4D5. Biochem J *398*, 23-36.

Conner, D. A. (2001). Mouse embryo fibroblast (MEF) feeder cell preparation. Curr Protoc Mol Biol *Chapter 23*, Unit 23 22.

Frank, R. (2002). The SPOT-synthesis technique. Synthetic peptide arrays on membrane supports--principles and applications. J Immunol Methods *267*, 13-26.

Jaworski, K., Ahmadian, M., Duncan, R. E., Sarkadi-Nagy, E., Varady, K. A., Hellerstein, M. K., Lee, H. Y., Samuel, V. T., Shulman, G. I., Kim, K. H., *et al.* (2009). AdPLA ablation increases lipolysis and prevents obesity induced by high-fat feeding or leptin deficiency. Nat Med *15*, 159-168.

Le Moan, N., Houslay, D. M., Christian, F., Houslay, M. D., and Akassoglou, K. (2011). Oxygen-dependent cleavage of the p75 neurotrophin receptor triggers stabilization of HIF-1alpha. Mol Cell *44*, 476-490.

Lesniewski, L. A., Hosch, S. E., Neels, J. G., de Luca, C., Pashmforoush, M., Lumeng, C. N., Chiang, S. H., Scadeng, M., Saltiel, A. R., and Olefsky, J. M. (2007). Bone marrow-specific Cap gene deletion protects against high-fat diet-induced insulin resistance. Nat Med *13*, 455-462.

Passino, M. A., Adams, R. A., Sikorski, S. L., and Akassoglou, K. (2007). Regulation of hepatic stellate cell differentiation by the neurotrophin receptor p75NTR. Science *315*, 1853-1856.

Sin, Y. Y., Edwards, H. V., Li, X., Day, J. P., Christian, F., Dunlop, A. J., Adams, D. R., Zaccolo, M., Houslay, M. D., and Baillie, G. S. (2011). Disruption of the cyclic AMP phosphodiesterase-4 (PDE4)-HSP20 complex attenuates the beta-agonist induced hypertrophic response in cardiac myocytes. J Mol Cell Cardiol *50*, 872-883.

Solinas, G., Vilcu, C., Neels, J. G., Bandyopadhyay, G. K., Luo, J. L., Naugler, W., Grivennikov, S., Wynshaw-Boris, A., Scadeng, M., Olefsky, J. M., and Karin, M. (2007). JNK1 in hematopoietically derived cells contributes to diet-induced inflammation and insulin resistance without affecting obesity. Cell Metab *6*, 386-397.

Tran, T. T., Yamamoto, Y., Gesta, S., and Kahn, C. R. (2008). Beneficial effects of subcutaneous fat transplantation on metabolism. Cell Metab *7*, 410-420.

Viswanadha, S., and Londos, C. (2006). Optimized conditions for measuring lipolysis in murine primary adipocytes. J Lipid Res *47*, 1859-1864.